Type II seesaw model: Searching for the LHC-elusive low-mass triplet Higgs bosons at e^-e^+ colliders

Saiyad Ashanujjaman,[1,2,*] Kirtiman Ghosh,[1,2,†] and Katri Huitu[3,‡]

[1]*Institute of Physics, Bhubaneswar, Sachivalaya Marg, Sainik School, Bhubaneswar 751005, India*
[2]*Homi Bhabha National Institute, Training School Complex, Anushakti Nagar, Mumbai 400094, India*
[3]*Department of Physics, and Helsinki Institute of Physics, University of Helsinki, P.O. Box 64, FI-00014 Helsinki, Finland*

(Received 2 June 2022; accepted 23 September 2022; published 28 October 2022)

While the tripletlike Higgses up to a few hundred GeV masses are already excluded for a vast region of the model parameter space from the LHC searches, strikingly, there is a region of this parameter space that is beyond the reach of the existing LHC searches, and doubly/singly charged and neutral Higgses as light as 200 GeV or even lighter are allowed by the LHC data. We study several search strategies targeting different parts of this LHC elusive parameter space at two configurations of e^-e^+ colliders—500 GeV and 1 TeV center of mass energies. We find that a vast region of this parameter space could be probed with 5σ statistical significance indicating discovery with the early e^-e^+ colliders' data.

DOI: 10.1103/PhysRevD.106.075028

I. INTRODUCTION

Among several observational and theoretical lacunae of the Standard Model (SM), the discovery of neutrino oscillations—necessitating the neutrinos to be massive—has provided arguably the most irrefutable reason for going beyond the SM. The widely studied type II seesaw model [1–6], one of the three UV completions of the so-called Weinberg operator [7] at the tree level [8], extending the SM with an $SU(2)_L$ triplet scalar field with hypercharge $Y = 1$ offers a well-founded rationale for the observed neutrino masses and mixings.

The copious production of the tripletlike physical Higgses, viz. doubly and singly charged Higgses ($H^{\pm\pm}$ and $H^{\pm}$) and CP-even and CP-odd neutral Higgses (H^0 and A^0),[1] and their eventual decays to the SM fermions and bosons offer interesting ways to probe them directly at colliders. The phenomenology of these states, in particular, the doubly charged ones, has been studied extensively at the Large Hadron Collider (LHC) [9–42], e^-e^+ colliders [43–48], and e^-p collider [49,50]; see Refs. [51,52] for comprehensive reviews. The observations being consistent with the SM expectations, several LHC searches performed by the CMS and ATLAS collaborations have put stringent limits on new states [53–62]. For $H^{\pm\pm}$ decaying exclusively into a same-sign lepton pair, the CMS multilepton search in Ref. [58] has set a limit of 535–820 GeV. The ATLAS multilepton search in Ref. [59] has set a limit of 770–870 GeV and 450 GeV for $H^{\pm\pm}$ decaying, respectively, 100% and 10% into a same-sign light lepton pair. For $H^{\pm\pm}$ decaying exclusively into a same-sign W-boson pair, the ATLAS search in Ref. [62] has set a limit of 350 GeV and 230 GeV, respectively, for the pair and associated production modes. Reference [42], incorporating all the relevant productions and decays for the tripletlike Higgses, has estimated the most stringent limit on $m_{H^{\pm\pm}}$ for a vast model parameter space by recasting several searches by CMS and ATLAS as well as studying a new multilepton search. They have projected a limit of 640(1490) GeV for $H^{\pm\pm}$ decaying into a pair of same-sign W-bosons (leptons) at 3000 fb^{-1} configuration of the LHC (HL-LHC).

Also, CMS and ATLAS have performed several searches for heavy neutral as well as singly charged resonances decaying into a pair of SM bosons or leptons [63–80]. Considering their production through gluon-gluon and vector-boson fusion processes, these searches have put limits on their production cross sections folded with the

*saiyad.a@iopb.res.in
†kirti.gh@gmail.com
‡katri.huitu@helsinki.fi

[1]While $H^{\pm\pm}$ is purely a triplet component, the rest are admixtures of doublet and triplet components. On account of the small mixings between them—occasioned by the SM Higgs-to-diphoton decay rate at the LHC as well as the small v_t constraint from the ρ parameter measurement from the electroweak precision data (EWPD), the states with admixtures dominated by the triplet components are dubbed *tripletlike*.

corresponding branching ratio. However, on account of the small mixing between the triplet Higgs and the SM doublet Higgs, $H^{\pm}$, H^0, and A^0 are fermiophobic to all charged leptons and quarks [81,82], and their production through such processes thereby are of little consequence. Therefore, suppressed production rates for these scalars immune them from receiving any constraints from these conventional LHC searches.

Understandably, with the LHC searches being designed to probe specific parts of the parameter space defined by the doubly charged Higgs mass ($m_{H^{\pm\pm}}$), the mass-splitting between the doubly and singly charged Higgses ($\Delta m = m_{H^{\pm\pm}} - m_{H^{\pm}}$) and the triplet vacuum expectation value (v_t), the resulted limits are not applicable for the entire parameter space. It has been shown in Ref. [42] that while the tripletlike Higgses up to a few hundred GeV masses are excluded for $\Delta m = 0$ and $\Delta m < 0$ from the LHC searches, strikingly, there is a region of the parameter space—with large enough positive Δm and moderate v_t—that is beyond the reach of the existing LHC searches, and Higgses as light as 200 GeV or even lighter are allowed by the LHC data. The challenges in probing this part of the parameter space at the LHC arise because the charged Higgses decay exclusively to the neutral ones and off-shell W-bosons resulting in soft hadrons or leptons, which are challenging to reconstruct at the LHC. Thus, charged Higgses' productions only enhance the production of neutral Higgses, which then decay to $\nu\nu$ or $b\bar{b}, t\bar{t}, ZZ, Zh, hh$, thereby resulting in final states that are challenging to probe at the LHC owing to the towering background. However, future lepton colliders [83–86] are expected to have better prospects for probing this region of the parameter space owing to a cleaner environment. This work studies several search strategies targeting different parts of the above-mentioned LHC elusive parameter space at future e^-e^+ colliders. To this end, we consider two configurations of e^-e^+ colliders—500 GeV and 1 TeV center of mass energies ($\sqrt{s}$).

The rest of this work is structured as follows. In Sec. II, we briefly discuss the type II seesaw model and the productions and decays of the tripletlike Higgses. We perform a comprehensive collider analysis for them in several final states at the 500 GeV and 1 TeV e^-e^+ colliders in Sec. III. Finally, we summarize in Sec. IV.

II. THE HIGGS TRIPLET

In addition to the SM field content, the type II seesaw model employs a $SU(2)_L$ triplet scalar field with $Y = 1$:

$$\Delta = \begin{pmatrix} \Delta^+/\sqrt{2} & \Delta^{++} \\ \Delta^0 & -\Delta^+/\sqrt{2} \end{pmatrix}.$$

The scalar potential involving Δ and the SM Higgs doublet $\Phi = (\Phi^+ \Phi^0)^T$ is given by [82]

$$\begin{aligned} V(\Phi,\Delta) = &-m_\Phi^2 \Phi^\dagger\Phi + \frac{\lambda}{4}(\Phi^\dagger\Phi)^2 + m_\Delta^2 \mathrm{Tr}(\Delta^\dagger\Delta) \\ &+ [\mu(\Phi^T i\sigma^2 \Delta^\dagger \Phi) + \mathrm{H.c.}] + \lambda_1(\Phi^\dagger\Phi)\mathrm{Tr}(\Delta^\dagger\Delta) \\ &+ \lambda_2[\mathrm{Tr}(\Delta^\dagger\Delta)]^2 + \lambda_3 \mathrm{Tr}[(\Delta^\dagger\Delta)^2] + \lambda_4 \Phi^\dagger \Delta\Delta^\dagger \Phi, \end{aligned}$$

where m_Φ^2, m_Δ^2, and μ are the mass parameters, λ and λ_i ($i = 1, \ldots, 4$) are the dimensionless quartic couplings. The neutral components of Φ and Δ can be parametrized as $\Phi^0 = (v_d + h + iZ_1)/\sqrt{2}$ and $\Delta^0 = (v_t + \xi + iZ_2)/\sqrt{2}$, where v_d and v_t are their respective vacuum expectation values (VEVs) with $\sqrt{v_d^2 + 2v_t^2} = 246$ GeV. After the electroweak symmetry is broken, the degrees of freedom carrying identical electric charges mix, thereby resulting in several physical Higgs states:

(i) the neutral states Φ^0 and Δ^0 mix into two CP-even states (h and H^0) and two CP-odd states (G^0 and A^0),
(ii) the singly charged states $\Phi^\pm$ and $\Delta^\pm$ mix into two mass states $G^\pm$ and $H^\pm$,
(iii) the doubly charged gauge state $\Delta^{\pm\pm}$ is aligned with its mass state $H^{\pm\pm}$.

The mass states G^0 and $G^\pm$ are the so-called *would-be* Nambu-Goldstone bosons eaten by the longitudinal modes of Z and $W^\pm$, and the rest of them are massive with h being identified as the 125 GeV resonance observed at the LHC.

The Yukawa interaction $Y^\nu_{ij} L_i^T C i\sigma^2 \Delta L_j$ of the triplet Higgs with the SM lepton doublet leads to the nonzero masses for the neutrinos after the electroweak symmetry breaking (Y^ν is a 3×3 symmetric complex matrix, i and j are the generation indices, and C is the charge-conjugation matrix):

$$m_\nu = \sqrt{2} Y^\nu v_t.$$

Consequently, Y^ν is determined by the neutrino oscillation parameters up to the triplet VEV. In this work, we take the best fit values for the neutrino oscillation parameters from Ref. [87], except for the Dirac and Majorana phases which we set to zero for simplicity.

In this model, there are only three phenomenologically relevant parameters, namely the doubly charged Higgs mass ($m_{H^{\pm\pm}}$), the mass-splitting between the doubly and singly charged Higgses ($\Delta m = m_{H^{\pm\pm}} - m_{H^\pm}$), and v_t. The tripletlike singly charged and neutral Higgs masses are given by

$$m_{H^\pm} = m_{H^{\pm\pm}} - \Delta m \tag{1}$$

and

$$m_{H^0/A^0} \approx \sqrt{m_{H^{\pm\pm}}(m_{H^{\pm\pm}} - 4\Delta m)}. \tag{2}$$

For the sake of completeness, we briefly mention the relevant constraints on them.

(i) The value of the ρ parameter from the EWPD [88] leads to an upper bound of $\mathcal{O}(1)$ GeV on v_t.

(ii) The EWPD observables, viz. S, T, and U parameters robustly constrain the mass-splittings requiring $|\Delta m| \lesssim 40$ GeV [39,89–91].

(iii) The SM Higgs-to-diphoton decay rate at the LHC constrains the CP-even Higgs mixing angle α: $|\sin\alpha| \lesssim 0.3$ at 95% confidence level [39].

(iv) The upper limits on the lepton flavor violating decays $\mu^- \to e^-\gamma$ [92] and $\mu^- \to e^+e^-e^-$ [93] tightly constrain the $v_t - m_{H^{\pm\pm}}$ parameter space [94–96]:

$$v_t \gtrsim \mathcal{O}(10^{-9})\ \text{GeV} \times \frac{1\ \text{TeV}}{m_{H^{\pm\pm}}}.$$

(v) For $\Delta m = 0$ and large (small) v_t, $H^{\pm\pm}$ with masses below 420 (955) GeV are excluded from the LHC searches, while the HL-LHC projection is 640 (1490) GeV. For large enough negative Δm and moderate v_t, the exclusion limit (HL-LHC projection) extends up to 1115 (1555) GeV. However, for large enough positive Δm and moderate v_t, tripletlike Higgses as light as 200 GeV or even lighter are allowed by the LHC data [42].

The triplet Higgses can be pair produced aplenty at e^-e^+ colliders through s-channel γ/Z exchanges [46][2]:

$$e^-e^+ \to H^{++}H^{--}, H^+H^-, H^0A^0.$$

We evaluate the leading order production cross sections using the SARAH 4.14.4 [97,98] generated UFO [99] modules in MadGraph5_aMC_v2.7.3 [100,101]. Figure 1 shows the total production cross sections for the tripletlike Higgses as a function of $m_{H^{\pm\pm}}$ for $\Delta m = 30$ GeV[3] at both the 500 GeV and 1 TeV e^-e^+ colliders.

After being produced, the tripletlike Higgses decay either into a lighter tripletlike Higgs and an off-shell W-boson or into a pair of SM particles. For the model parameter space of our interest—with large enough positive Δm and moderate v_t—$H^{\pm\pm}$ and $H^{\pm}$ undergo the former decay [21,42,81], thereby enhancing the productions of H^0 and A^0 effectively. Finally, H^0 and A^0 decay into a pair of neutrinos or/and $b\bar{b}, t\bar{t}, ZZ, Zh, hh$. In Fig. 2, we present their branching fractions as a function of v_t for different values of $m_{H^{\pm\pm}}$—200, 250, 350, and 450 GeV with $\Delta m = 30$ GeV. As these plots suggest, the dominance of a decay mode over the others depends, naturally, on their mass and v_t.

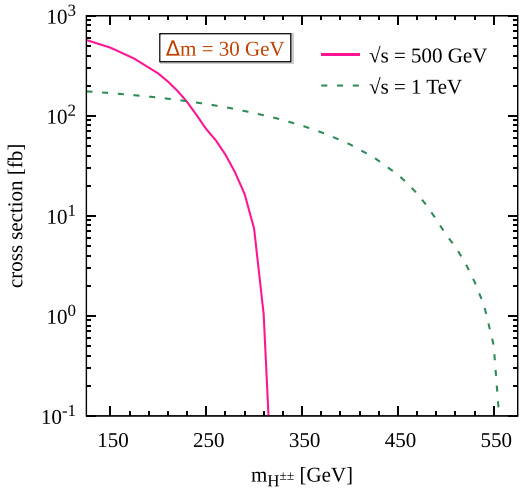

FIG. 1. Total production cross sections for the tripletlike Higgses at the 500 GeV and 1 TeV e^-e^+ colliders.

III. COLLIDER PHENOMENOLOGY

The abundant production of the tripletlike Higgses followed by their eventual decays to the SM particles will lead to various final state signatures at e^-e^+ colliders. For the parameter space of our interest with $\Delta m = 30$ GeV and $v_t \sim \mathcal{O}(10^{-6})$–$\mathcal{O}(10^{-3})$ GeV, both $H^{\pm\pm}$ and $H^{\pm}$ decay to H^0/A^0 and off-shell W-bosons, then the decays of H^0/A^0 proceed through different modes depending on their mass and v_t (see Fig. 2). Consequently, different parts of this parameter space concern different decay modes of H^0/A^0:

(1) $v_t \lesssim \mathcal{O}(10^{-4})$ GeV: Both H^0 and A^0 decay invisibly to neutrinos irrespective of their mass, with the visible objects coming only from the off-shell W-bosons. Consequently, the final state comprises soft leptons and/or jets plus p_T^{miss}.

(2) $v_t \sim \mathcal{O}(10^{-4}) - \mathcal{O}(10^{-3})$ GeV and $m_{H^{\pm\pm}} \lesssim 290$ GeV: One of A^0 and H^0 dominantly decays to $\nu\nu$, and the other decays to WW or Zh, thereby resulting in multiple jets in the final state.

(3) $v_t \gtrsim \mathcal{O}(10^{-4})$ GeV and $m_{H^{\pm\pm}} \lesssim 250$ GeV: A^0 dominantly decays to $b\bar{b}$, and H^0 decays to $\nu\nu$, $b\bar{b}$ or WW so that the final state includes at least two b-jets in addition to other jets or leptons if any.

(4) $v_t \gtrsim \mathcal{O}(10^{-4})$ GeV and $m_{H^{\pm\pm}} \gtrsim 250$ GeV: H^0 and A^0 decay dominantly into hh/ZZ and Zh, respectively. Consequently, the final state comprises $hhhZ$ or $ZZZh$ in the final state, in addition to the off-shell W-bosons coming from the cascade decays of $H^{\pm\pm}$ and $H^{\pm}$. Further, the hadronic decays of the h/Z-bosons results in up to eight jets (with two to six of these being b-jets) but for the soft leptons/jets coming from the off-shell W-bosons.

[2]They can also be single or pair produced via vector-boson fusion processes with two associated forward leptons at e^-e^+ colliders. However, we do not consider these due to their small contribution.

[3]For the sake of definiteness, we consider a mass-splitting of 30 GeV for the rest of this work, then touch on the case for a smaller mass-splitting in Sec. IV.

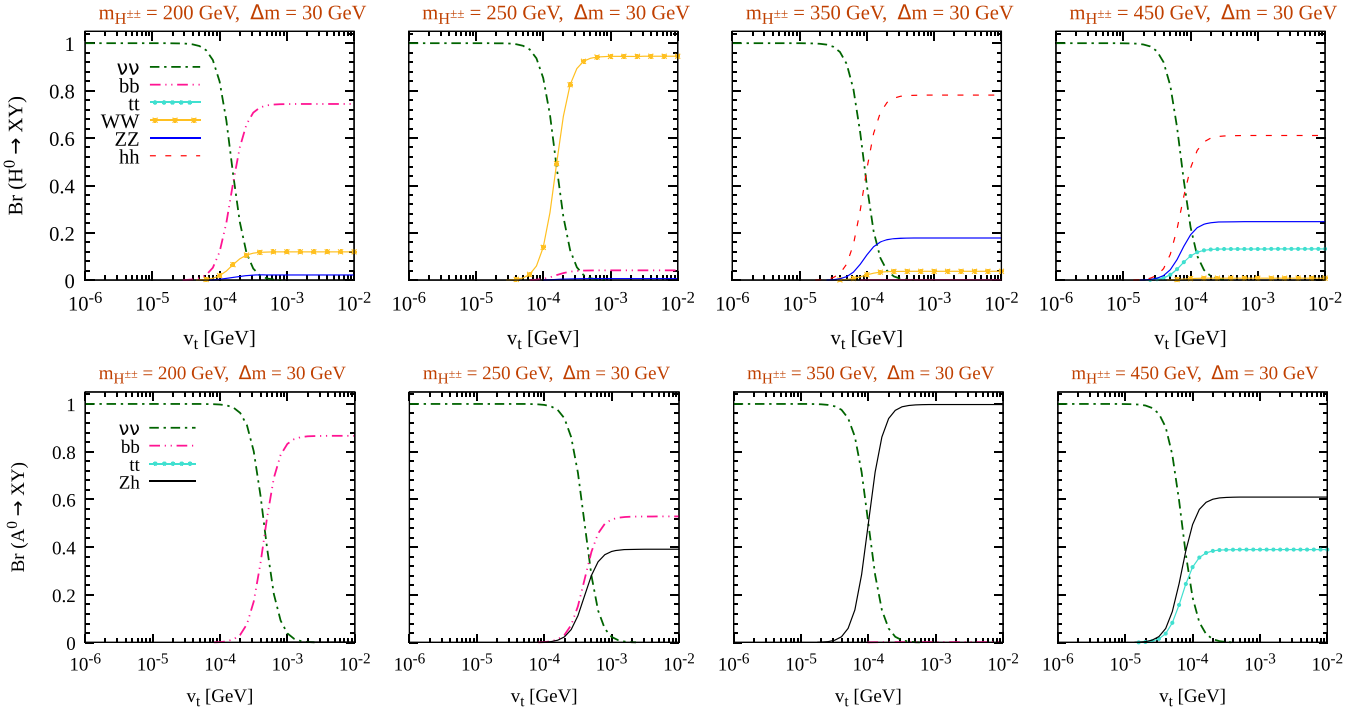

FIG. 2. Branching fractions for the tripletlike *CP*-even (top panel) and *CP*-odd (bottom panel) neutral Higgses.

Led the way by the decay patterns of H^0 and A^0 as discussed above (also, see Fig. 2), we define four signal regions (SRs) targeting different parts of the above-mentioned parameter space. These SRs are summarized in Table I, and the corresponding benchmark points relevant for the subsequent discussion are summarized in Table II. Before going into the SR-specific selection, we briefly describe the reconstruction and selection of various physics objects.

A. Object reconstruction and selection

We use MadGraph5_aMC_v2.7.3 [100,101] to simulate parton-level events for both signals and backgrounds. We pass those events into PYTHIA 8.2 [102] to simulate subsequent decays for the unstable particles, initial and final state radiations, showering, fragmentation, and hadronization. Finally, we pass them into DELPHES 3.4.2 [103] with the default card for the International Linear Collider for simulating detector effects as well as reconstructing various

TABLE I. SRs targeting different parts of the parameter space.

	Parameter space of interest				
SR	v_t (GeV)	Δm (GeV)	$m_{H^{\pm\pm}}$ (GeV)	Final state of interest	$\sqrt{s}$ (GeV)
SR1	$\gtrsim\mathcal{O}(10^{-4})$	30	$\lesssim$250	$\geq 2b$-jets + anything	500
SR2	$\mathcal{O}(10^{-4}) - \mathcal{O}(10^{-3})$	30	$\lesssim$290	$\geq$3 jets + p_T^{miss}	500
SR3	$\lesssim\mathcal{O}(10^{-4})$	30	$\lesssim$250(500)	soft leptons/jets	500(1000)
SR4	$\gtrsim\mathcal{O}(10^{-4})$	30	$\gtrsim$250	$\geq$7 jets (with $\geq 2b$-jets)	1000

TABLE II. Benchmark points used for different SRs.

	Benchmark points					
SR	Name	$m_{H^{\pm\pm}}$ (GeV)	Δm (GeV)	v_t (GeV)	$m_{H^{\pm}}$ (GeV)	m_{H^0/A^0} (GeV)
SR1	*BP1*	230	30	3×10^{-4}	200	165
SR2	*BP2*	260	30	3×10^{-4}	230	195
SR3	*BP3* (*BP4*)	240 (425)	30	10^{-5}	210 (395)	175 (363)
SR4	*BP5*	375	30	3×10^{-4}	345	312

physics objects, viz. photons, electrons, muons, and jets. Jets are reconstructed using the *anti-k_T algorithm* [104] with a characteristic radius 0.4 in FastJet 3.3.2 [105]. Jets (leptons, i.e. electrons and muons, and photons) are required to be within the pseudorapidity range $|\eta| < 2.4(2.5)$ and have a transverse momentum $p_T > 10(5)$ GeV. Further, muons (photons and electrons) are required to be isolated, and this is ensured by demanding the scalar sum of the p_Ts of all other objects lying within a cone of radius 0.5 around it to be smaller than 15%(12%) of its p_T. Such stringent isolation requirements significantly suppress the reducible backgrounds. Finally, the missing transverse momentum vector $\vec{p}_T^{\,\text{miss}}$ (with magnitude p_T^{miss}) is estimated from the momentum imbalance in the transverse direction associated to all reconstructed objects in an event.

B. SM Backgrounds

While different SM processes serve as the main background for different SRs, for the sake of completeness, we consider all the relevant backgrounds across the SRs. These include diboson (VV with V denoting the gauge bosons), triboson (VVV) and tetraboson ($VVVV$) productions, Higgsstrahlung processes (Vh, VVh, Vhh, $t\bar{t}h$), multitop production ($t\bar{t}$, $t\bar{t}t\bar{t}$), top-pair production in association with gauge bosons ($t\bar{t}V$, $t\bar{t}VV$), dilepton production, and multijet production. We have generated these backgrounds at least 1000 fb^{-1} luminosity worth of data at the 500 GeV (1 TeV) e^-e^+ collider: 10^6 events for $b\bar{b}$, $t\bar{t}$, and VVV each; 10^7 (3×10^6) events for VV; and 10^5 events for other relevant processes each.

C. SR-specific event selection

We now briefly discuss the SR-specific selection criteria that would significantly suppress the background without impinging much on the signal. To achieve this, we use various kinematic distributions as a guiding premise.

1. SR1: $v_t \gtrsim \mathcal{O}(10^{-4})$, $\Delta m \sim 30$, $m_{H^{\pm\pm}} \lesssim 250$ GeV

In this SR, A^0 dominantly decays to $b\bar{b}$, and H^0 decays to $\nu\nu$, $b\bar{b}$, or WW so that the final state includes at least two b-jets in addition to other jets or leptons if any. We require at least two of the jets to be b-tagged. The invariant mass distribution of these two b-tagged jets are expected to peak at m_{H^0/A^0}. The SM processes $t\bar{t}$ and $b\bar{b}$ serve as the main irreducible backgrounds for this final state. In Fig. 3, we display two normalized kinematic distributions for the signal and background events at the 500 GeV e^-e^+ collider. The signal events are shown for a benchmark point *BP1*: $m_{H^{\pm\pm}} = 230$ GeV, $\Delta m = 30$ GeV, and $v_t \sim 3 \times 10^{-4}$ GeV. The left plot shows the distribution for the angle between the two b-tagged jets ($\cos\theta_{bb}$). In case of more than two b-tagged jets, the pair with maximum separation in the azimuth plane is considered. The background boasts a peak around $\cos\theta_{bb} = -1$ with

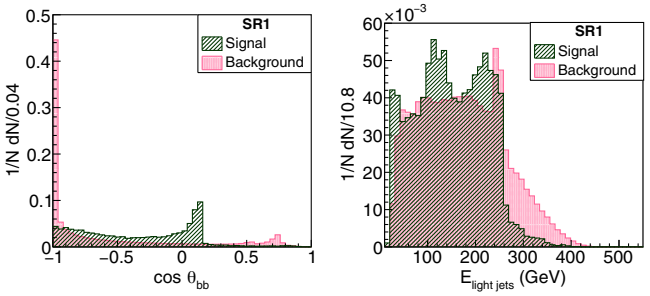

FIG. 3. Normalized kinematic distributions for the signal (*BP1*) and background at the 500 GeV e^-e^+ collider. Left: $\cos\theta_{bb}$ and right: $E_{\text{light jets}}$.

the most dominant contribution coming from $b\bar{b}$ events with the pair of b-jets emanating back-to-back. Displayed in the right plot is the distribution of the sum of all non b-tagged jet energies ($E_{\text{light jets}}$). To improve the signal-to-background ratio, we impose the following selection cuts:

$$\cos\theta_{bb} \in [-0.96, 0.4] \quad \text{and} \quad E_{\text{light jets}} < 250 \text{ GeV}.$$

The sensitivity of this search is increased by dividing the selected events into 8 bins in the range [100,300] GeV using the invariant mass of the two b-tagged jets (m_{bb}) as the final discriminating variable between the signal and background (see Fig. 4). As we expected, the m_{bb} distribution peaks in the 150–175 GeV bin, thereby reconstructing the tripletlike neutral Higgses.

2. SR2: $v_t \sim \mathcal{O}(10^{-4}) - \mathcal{O}(10^{-3})$, $\Delta m \sim 30$, $m_{H^{\pm\pm}} \lesssim 290$ GeV

In this SR, one of A^0 and H^0 dominantly decays to $\nu\nu$, and the other decays to WW or Zh. We require at least three jets in the final state. To suppress the background contributions from $t\bar{t}$ and $b\bar{b}$ processes, we apply a b-jet veto. We display some normalized kinematic distributions for the

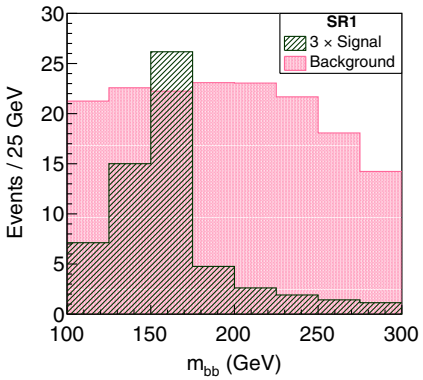

FIG. 4. m_{bb} distribution for the signal (*BP1*) and background. The events are weighted for 1 fb^{-1} luminosity at the 500 GeV e^-e^+ collider.

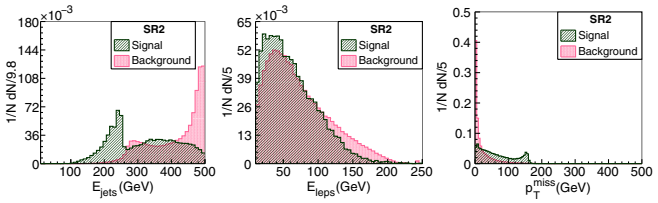

FIG. 5. Normalized kinematic distributions for the signal (*BP2*) and background at the 500 GeV e^-e^+ collider. Left: $E_{\rm jets}$, middle: $E_{\rm leps}$, and right: $p_T^{\rm miss}$.

signal and background events at the 500 GeV e^-e^+ collider in Fig. 5. The signal events are shown for a benchmark point *BP2*: $m_{H^{\pm\pm}} = 260$ GeV, $\Delta m = 30$ GeV, and $v_t \sim 3 \times 10^{-4}$ GeV. The left (middle) plot shows the distribution for the sum of all jet (lepton) energies, $E_{\rm jets}$ ($E_{\rm leps}$). As for the $E_{\rm jets}$ distribution for the background events, it is almost a monotonically rising one, peaking at $\sqrt{s}$, with most of the contributions coming from WW and $t\bar{t}$ productions. Whereas for the signal events, it is a wide one, extending up to $\sqrt{s}$ with a peak at $\sqrt{s}/2$. Also displayed, in the right plot, is the $p_T^{\rm miss}$ distribution. For the signal, this distribution is almost flat, extending beyond 150 GeV. This is effectuated by one of the two tripletlike scalars' decay to hadronic final state, with the other decaying invisibly. On the contrary, for the background events, it is almost a monotonically falling one, falling sharply at very low $p_T^{\rm miss}$. Guided by these kinematic distributions, we impose the following selection cuts to improve the signal-to-background ratio:

$$E_{\rm jets} < 260\,{\rm GeV}, \quad E_{\rm leps} < 120\,{\rm GeV} \quad \text{and} \quad p_T^{\rm miss} > 40\,{\rm GeV}.$$

Though the adoption of the cut on $E_{\rm jets}$ impinges on the signal strength, this significantly increases the signal-to-background ratio, owing to a much diminished background.

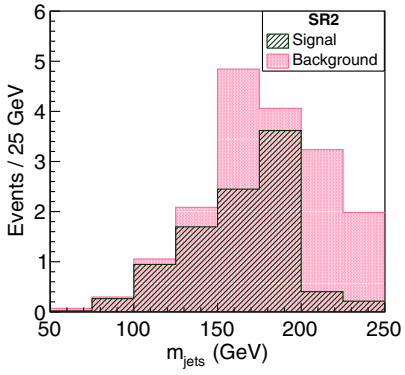

FIG. 6. $m_{\rm jets}$ distribution for the signal (*BP2*) and background. The events are weighted for 1 fb^{-1} luminosity at the 500 GeV e^-e^+ collider.

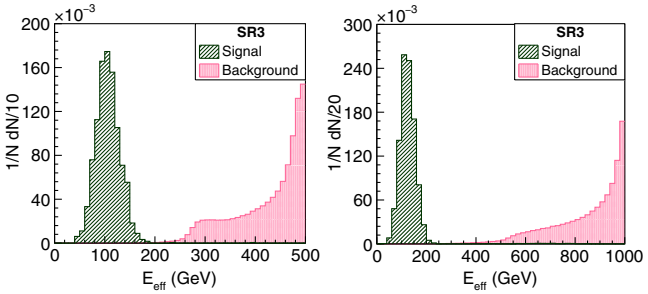

FIG. 7. Normalized $E_{\rm eff}$ distribution for the signal (left: *BP3*, right: *BP4*) and background at the 500 GeV (left) and 1 TeV (right) e^-e^+ colliders.

To enhance the sensitivity of this search further, the selected events are distributed over 8 bins in the range [50,250] GeV using the invariant mass of all jets, $m_{\rm jets}$ (see Fig. 6).

3. SR3: $v_t \lesssim \mathcal{O}(10^{-4})$, $\Delta m \sim 30$, and $m_{H^{\pm\pm}} \lesssim 250(500)$ GeV

In this SR, $H^{\pm\pm}$ and $H^{\pm}$ decay to H^0/A^0 and off-shell W-bosons. While H^0 and A^0 decay to neutrinos, the off-shell W-bosons decay to soft leptons/jets, thereby resulting in soft leptons/jets plus $p_T^{\rm miss}$ in the final state.[4] We require at least three soft leptons and/or jets in the final state. In Fig. 7, we display the normalized kinematic distributions for $E_{\rm eff} = E_{\rm jets} + E_{\rm leps} + p_T^{\rm miss}$ for the signal and background events at the 500 GeV and 1 TeV e^-e^+ colliders. The signal events are shown for a benchmark point *BP3* (*BP4*): $m_{H^{\pm\pm}} = 240(425)$ GeV, $\Delta m = 30$ GeV, and $v_t \sim 10^{-5}$ GeV at the 500 GeV (1 TeV) collider. For the signal, this distribution boasts a peak around 100 GeV, thereafter falling sharply. This is occasioned by the softness of the leptons/jets stemming from the off-shell W-bosons. On the other hand, for the background events, it is almost a monotonically rising one, peaking at $\sqrt{s}$, with bulk of the contributions coming from WW, ZZ, and $t\bar{t}$ productions. Guided by these distributions, we apply the following selection cut to ameliorate the signal-to-background ratio:

$$E_{\rm eff} < 200(250)\ {\rm GeV\ for\ the\ 500\ GeV\ (1\ TeV)\ collider}.$$

[4]Note that $p_T^{\rm miss}$ is estimated against the transverse momentum imbalance associated to the (visible) reconstructed objects in an event. Because of the more likely hard jets in the *SR2* final state, $p_T^{\rm miss}$ tend to be much larger than that for *SR3*, in which the leptons/jets emanating from the off-shell W-bosons are more likely soft owing to the small triplet mass-splitting. Consequently, while a cut on $p_T^{\rm miss}$ is found to be effective in enhancing the signal-to-background ratio for *SR2*, this is not the case for *SR3*.

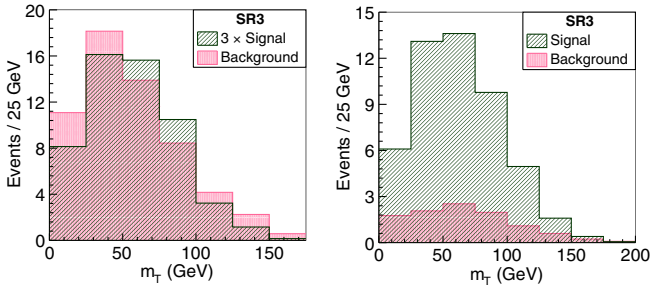

FIG. 8. m_T distribution for the signal (left: *BP3*, right: *BP4*) and background. The events are weighted for 10 fb^{-1} luminosity at the 500 GeV (left) and 1 TeV (right) e^-e^+ colliders.

Finally, the selected events are distributed over 7 bins in the range [0,175] GeV using the transverse mass m_T (see Fig. 8), where m_T is defined as

$$m_T^2 = 2p_T^{\rm miss} p_T^{\rm vis}(1 - \cos\Delta\phi_{\vec{p}_T^{\rm miss},\vec{p}_T^{\rm vis}}),$$

where $\vec{p}_T^{\rm vis}$ (with magnitude $p_T^{\rm vis}$) is the vector sum of the transverse momenta of all leptons and jets, and $\Delta\phi_{\vec{p}_T^{\rm miss},\vec{p}_T^{\rm vis}}$ is the azimuthal separation between $\vec{p}_T^{\rm miss}$ and $\vec{p}_T^{\rm vis}$.

4. SR4: $v_t \gtrsim \mathcal{O}(10^{-4})$, $\Delta m \sim 30$, $m_{H^{\pm\pm}} \gtrsim 250$ GeV

In this SR, H^0 and A^0 decay dominantly into hh/ZZ and Zh, respectively. Thus, we have $hhhZ$ or $ZZZh$ in the final state, in addition to the off-shell W-bosons coming from the cascade decays of $H^{\pm\pm}$ and $H^{\pm}$. The hadronic decays of the h/Z-bosons result in up to eight jets but for the soft leptons/jets coming from the off-shell W-bosons. We require at least seven jets in the final state, with at least two of them to be b-tagged. This requirement reduces the background contributions from the diboson and QCD jets (in particular, $b\bar{b}+$ jets) production processes to a negligible level, while keeping only a small fraction of contributions from the triboson and multitop production processes. Brushing aside the soft jets/leptons from the off-shell W-bosons, there are as many as eight hard jets in the final state, in addition to the others coming from radiations and pileup interactions. On account of the high-multiplicity signature in the final state, it is particularly burdensome to correctly associate the reconstructed jets in an event with the elementary quarks of that event topology. This makes the kinematic reconstruction of H^0/A^0 very challenging. To resolve this *combinatorial problem*, we use the so-called χ^2-minimization method (see for example [106–108]), i.e. by enumerating and evaluating all possible permutations in an event,[5] we identify the *best* assignment through minimizing the objective function:

$$\chi^2 = \frac{(m_{j_1j_2} - m_{h/Z})^2}{m_{h/Z}^2} + \frac{(m_{j_3j_4} - m_{h/Z})^2}{m_{h/Z}^2} + \frac{(m_{j_5j_6} - m_{h/Z})^2}{m_{h/Z}^2} + \frac{(m_{j_7j_8} - m_{h/Z})^2}{m_{h/Z}^2} + \frac{(m_{j_1j_2j_3j_4} - m_{j_5j_6j_7j_8})^2}{\sigma_{H^0/A^0}^2},$$

and

$$\chi^2 = \frac{(m_{j_1j_2} - m_{h/Z})^2}{m_{h/Z}^2} + \frac{(m_{j_3j_4} - m_{h/Z})^2}{m_{h/Z}^2} + \frac{(m_{j_5j_6} - m_{h/Z})^2}{m_{h/Z}^2} + \frac{(m_{j_1j_2j_3j_4} - m_{j_5j_6j_7})^2}{\sigma'^2_{H^0/A^0}},$$

respectively, for eight and seven jet events with the jets being denoted as $j_1, j_2, \ldots, j_8$. This method enables us to pair eight (seven) jets in an event in order to reconstruct four (three) h/Z-boson as well as two (one) H^0/A^0 candidates. $m_{j_1j_2j_3j_4}$ and $m_{j_5j_6j_7j_8}$ ($m_{j_5j_6j_7}$) are the invariant masses of the jets associated with the decay products of H^0/A^0. The pair of H^0/A^0 being dissimilar in mass, the right assignment would correspond to the smaller difference between $m_{j_1j_2j_3j_4}$ and $m_{j_5j_6j_7j_8}$ ($m_{j_5j_6j_7}$). Likewise, $m_{j_1j_2}$, $m_{j_3j_4}$, $m_{j_5j_6}$, and $m_{j_7j_8}$ are the invariant masses of the jets associated with the hadronically decaying h/Z-bosons (with mass $m_{h/Z}$) from H^0/A^0. Finally, $\sigma_{H^0/A^0} = (m_{j_1j_2j_3j_4} + m_{j_5j_6j_7j_8})/2$ and $\sigma'_{H^0/A^0} = (m_{j_1j_2j_3j_4} + m_{j_5j_6j_7})/2$.

In Fig. 9, we display the normalized invariant mass distributions for the *best-assigned*[6] jet pairs for the signal and background events at the 1 TeV e^-e^+ collider. The signal events are shown for a benchmark point *BP5*: $m_{H^{\pm\pm}} = 375$ GeV, $\Delta m = 30$ GeV, and $v_t \sim 3 \times 10^{-4}$ GeV. These distributions exemplifies the effectiveness of the χ^2-minimization method.[7] The signal distributions boasts two peaks—one at m_Z and the other at m_h, thereby reconstructing the h/Z-bosons in the final state reasonably well. On the other hand, the background distribution boasts an additional peak at the W-mass—more pronounced than the other two, with the lion's share of the contributions accruing from the $t\bar{t}$ events. Finally, H^0/A^0 can be kinematically reconstructed from two pairs of jets in an event:

$$M_{\rm inv} = (m_{j_1j_2j_3j_4} + m_{j_5j_6j_7j_8})/2,$$

and

$$M_{\rm inv} = m_{j_1j_2j_3j_4},$$

[5]This method requires enumeration and evaluation of 315 (360) distinct permutations for eight (seven) jet events.

[6]The jet pairs' assignment corresponding to the minimum objective function is referred to as the *best* assignment.

[7]Note that not only does this method cost a considerable amount of time, but also it obscures the kinematic reconstruction owing to the incorrect assignments of the reconstructed jets to the particles in the event topology.

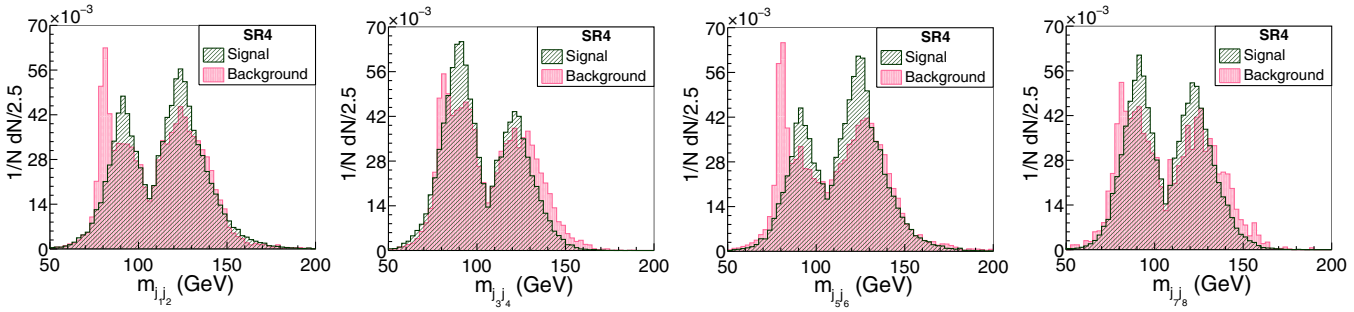

FIG. 9. Normalized invariant mass distributions for the *best-assigned* jet pairs for the signal (*BP5*) and background at the 1 TeV e^-e^+ collider.

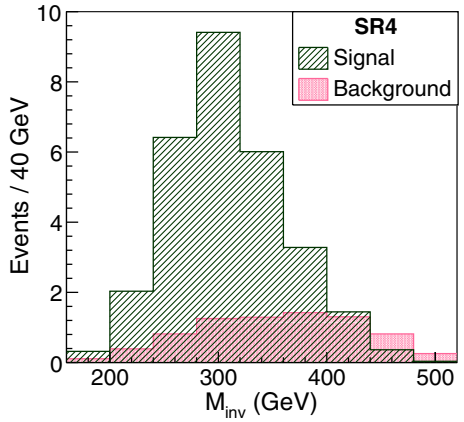

FIG. 10. $M_{\rm inv}$ distribution for the signal (*BP5*) and background. The events are weighted for 1 fb^{-1} luminosity at the 1 TeV e^-e^+ collider.

respectively, for 8 and 7 jet events. The sensitivity of this search is increased further by distributing the selected events into 9 bins in the range [160,520] GeV using the invariant mass $M_{\rm inv}$ (see Fig. 10). As we expected, the $M_{\rm inv}$ distribution peaks in the 280–320 GeV bin, thereby reconstructing the H^0/A^0.

D. Discovery reach

Next, we estimate the discovery reaches of the above SRs. For each signal model within a SR, the events passing the corresponding selection cuts discussed above are divided into several bins using a final discriminating variable between the signal and background (see Figs. 4, 6, 8, and 10). We feed the expected number of signal and background events along with the relative background uncertainties in these bins into a hypothesis tester named Profile Likelihood Number Counting Combination [109] which uses a library of C^{++} classes RooFit [110] in the ROOT 6.14.04 [111] environment to estimate the discovery significance of that signal model. In this hypothesis tester, all the signal/background bins are treated as independent channels, and the background uncertainties are included via the Profile Likelihood Ratio. We assume a flat 5% systematic uncertainty on the estimated background without going into the intricacy of estimating the same.[8]

We repeat the analysis described above not only for the benchmark points mentioned in Table II, but also for a vast range of v_t and $m_{H^{\pm\pm}}$ with $\Delta m = 30$ GeV. Note that, for a given SR, we use the same set of selection cuts across different values of v_t and $m_{H^{\pm\pm}}$. In Fig. 11,[9] we project the required luminosities for 5σ statistical significance for the discovery of the tripletlike Higgses as a function of their mass in different SRs at the 500 GeV and 1 TeV e^-e^+ colliders. Note that, for the 500 GeV configuration, the required luminosity increases sharply for *SR1* and *SR3* compared to *SR2*. This is because of a more enhanced background-to-signal for *SR2* compared to *SR1* and *SR3*, see Figs. 4, 6. and 8. For *SR2*, the requirements of *b*-jet veto

[8]The systematic uncertainties arise from several sources such as the luminosity measurements, the parton-shower modeling, the detector response modeling, the description of the differential cross sections, the higher-order QED and QCD corrections, etc. The systematic uncertainties in integrated luminosity measurement [112,113] as well as beam energy measurement [114–116] for future e^-e^+ colliders are estimated to be $\lesssim\mathcal{O}(0.1\%)$. A detailed study of potential systematic uncertainties for future e^-e^+ has not been performed yet. However, given the estimations of the past detectors at LEP [117–119], the assumption of flat 5% systematic uncertainty seems to be a reasonable one (if not conservative) [120,121].

[9]The SRs target different parts of the LHC elusive parameter space (see Table I and Fig. 2). For example, *SR4* requires at least seven jets in the final state, with at least two of them *b*-tagged, thereby concerning only the parameter space where H^0 and A^0 decay dominantly to hh/ZZ and Zh, respectively, i.e. $v_t \gtrsim \mathcal{O}(10^{-4})$ GeV and $m_{H^{\pm\pm}} \gtrsim 250$ GeV. Consequently, *SR4* is not apposite for the 500 GeV collider, but for the 1 TeV one. On the other hand, *SR2* concerns only the parameter space where one of A^0 and H^0 decays to $\nu\nu$ and the other decays to WW or Zh so that the final state includes at least three jets and considerably large missing transverse momentum, i.e. $v_t \sim \mathcal{O}(10^{-4}) - \mathcal{O}(10^{-3})$ GeV and $m_{H^{\pm\pm}} \lesssim 290$ GeV. As we see from Fig. 12, the 500 GeV collider is adept enough at probing this parameter space, and thus going for the 1 TeV configuration seems uncalled for. A similar argument follows for *SR1*. Therefore, while *SR1*, *SR2*, and *SR3* are pertinent for the 500 GeV collider, only *SR3* and *SR4* pertain to the 1 TeV configuration.

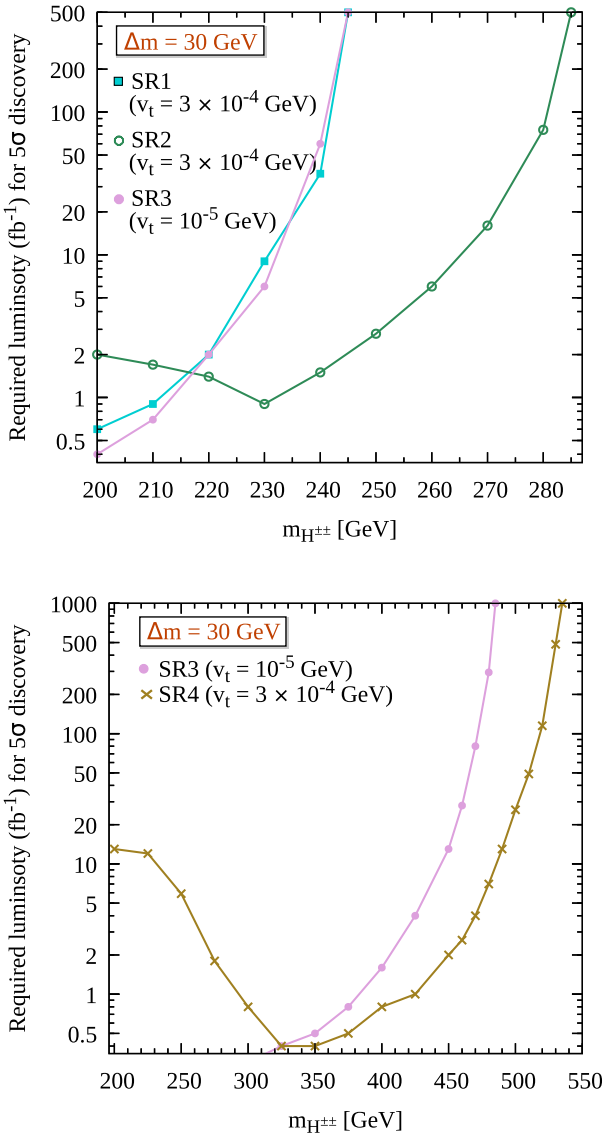

FIG. 11. Required luminosity for the 5σ discovery of the tripletlike Higgses in different SRs at the 500 GeV (top) and 1 TeV (bottom) e^-e^+ colliders.

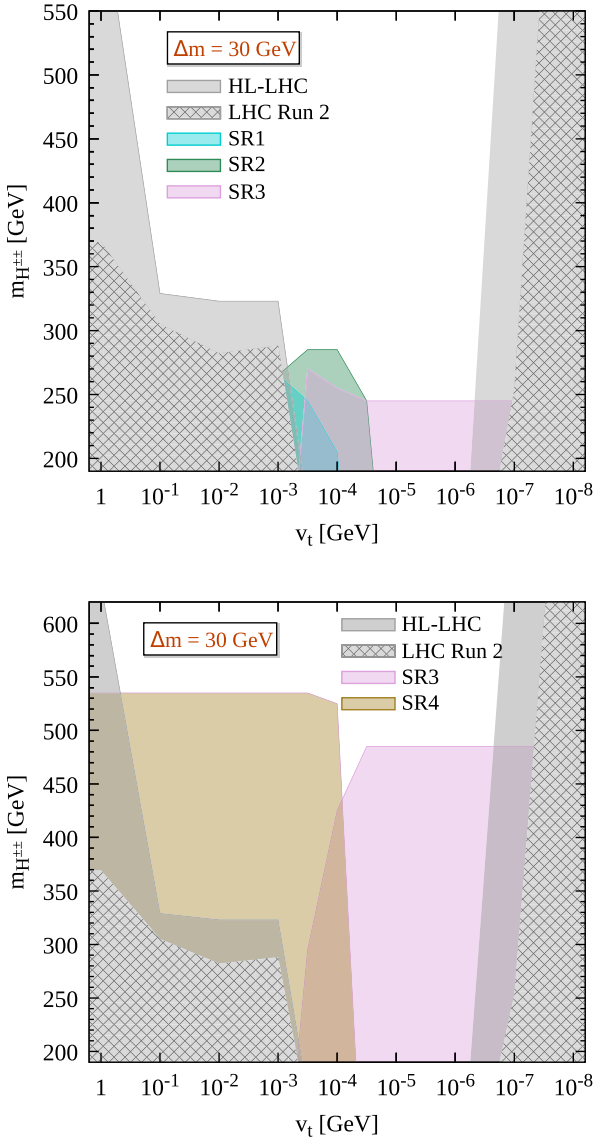

FIG. 12. Summary of the discovery reaches for the tripletlike Higgses in different SRs at the 500 GeV (top) and 1 TeV (bottom) e^-e^+ colliders with 500 and 1000 fb^{-1} luminosity data, respectively. The gray hatched and shaded regions are taken from Ref. [42]. See text for details.

and considerably large $p_T^{\rm miss}$ along with the others turn out to be very effective in vanquishing the relevant backgrounds (in particular, $t\bar{t}$ and VV) over the signal. On the contrary, owing to the requirement of two b-jets, the contamination from the $t\bar{t}$ background is inescapable for *SR1*. For *SR3*, the absence of any hard visible objects in the final state restrict further enhancement of the background-to-signal ratio.

Also shown, in Fig. 12, are the discovery reaches for the tripletlike Higgses in the v_t-$m_{H^{\pm\pm}}$ plane in different SRs at two configurations of e^-e^+ colliders—500 GeV and 1 TeV e^-e^+ colliders, respectively, with 500 and 1000 fb^{-1} luminosity data. For the sake of completeness, we also show the regions that are excluded from the LHC run 2 searches (gray hatched) as well as expected to be probed at the HL-LHC (gray shaded) [42]. For the 500 GeV e^-e^+ configuration with 500 fb^{-1} data, *SR2* has the maximum discovery reach of $m_{H^{\pm\pm}} \sim 285$ GeV because of its small background, whereas considerably large backgrounds for both *SR1* and *SR3* limit their reaches to $m_{H^{\pm\pm}} \sim 245$ GeV. Likewise, for the 1 TeV e^-e^+ configuration with 1000 fb^{-1} data, *SR4* is the most promising signal region with the discovery reach of $m_{H^{\pm\pm}} \sim 535$ GeV because of its small background and ability to kinematically reconstruct the neutral Higgses H^0/A^0, and *SR3* has a discovery reach of $m_{H^{\pm\pm}} \sim 485$ GeV.

IV. SUMMARY AND OUTLOOK

While the tripletlike Higgses up to a few hundred GeV masses are already excluded for a vast region of the model parameter space from the LHC searches, strikingly, there is a region of this parameter space—with large enough positive mass-splitting between the doubly and singly charged Higgses and moderate triplet Higgs scalar vacuum expectation value—that is beyond the reach of the existing LHC searches, and such Higgses as light as 200 GeV or even lighter are allowed by the LHC data [42]. In this region of the parameter space, the charged Higgses decay exclusively to the neutral ones and off-shell W-bosons. The latter results in soft leptons/jets that are challenging to reconstruct at the LHC. Furthermore, the neutral Higgses decay to neutrinos or $b\bar{b}, t\bar{t}, ZZ, Zh, hh$, thereby resulting in final states that are challenging to probe at the LHC owing to the towering SM backgrounds. However, owing to a cleaner environment, future lepton colliders are expected to have better prospects for probing this LHC elusive parameter space. In this work, we study several search strategies targeting different parts of this parameter space at future e^-e^+ colliders with 500 GeV and 1 TeV center of mass energies. We find that a vast region of this parameter space could be probed with 5σ statistical significance with the early e^-e^+ colliders' data. Furthermore, the tripletlike neutral Higgses could be kinematically reconstructed for a significant part of this parameter space, particularly those concerning the *SR1* and *SR4* signal regions.

In closing this section, a few comments are in order. (i) For the sake of definiteness, we have shown our findings for a mass-splitting of 30 GeV. However, the searches presented above would also be sensitive for smaller mass-splittings. Brushing aside a little quantitative difference in production cross sections for the tripletlike Higgses, the only major difference between a smaller mass-splitting (say, 10 GeV) and a larger one (say, 30 GeV) is that the leptons/jets stemming from the off-shell W-bosons would be softer. Note that only the search in *SR3* targets soft leptons/jets in the final state. Therefore, for a smaller mass-splitting, the $E_{\rm eff}$ distribution in Fig. 7 would shift towards lower values, thus allowing one to impose a stronger cut on it. While this would impinge only a little on the signal strength, the same would significantly enhance the signal-to-background ratio, primarily on account of a much reduced background. On the other hand, the searches in *SR1*, *SR2*, and *SR4* target hard jets/leptons stemming from the tripletlike Higgses' decays, thus these are almost independent of the mass-splitting. (ii) The *SR3* region of parameter space could also be probed by using a search with a photon and missing transverse momentum in the final state. Such final states suffer from a large irreducible background contributions from the t-channel W-exchange process $\nu\bar{\nu}\gamma$. Though this background could be reduced by a factor of a few by using polarized beams (positively polarized for e^- and negatively polarized for e^+), on account of the small signal strength occasioned by the requirement of an energetic photon, the discovery reach of such a search would be very limited.

ACKNOWLEDGMENTS

K. G. acknowledges support from the DST INSPIRE Research Grant [DST/INSPIRE/04/2014/002158] and SERB Core Research Grant [CRG/2019/006831].

[1] W. Konetschny and W. Kummer, Nonconservation of total lepton number with scalar bosons, Phys. Lett. **70B**, 433 (1977).
[2] T. P. Cheng and L.-F. Li, Neutrino masses, mixings and oscillations in SU(2) × U(1) models of electroweak interactions, Phys. Rev. D **22**, 2860 (1980).
[3] G. Lazarides, Q. Shafi, and C. Wetterich, Proton lifetime and fermion masses in an SO(10) model, Nucl. Phys. **B181**, 287 (1981).
[4] J. Schechter and J. W. F. Valle, Neutrino masses in SU(2) × U(1) theories, Phys. Rev. D **22**, 2227 (1980).
[5] R. N. Mohapatra and G. Senjanovic, Neutrino masses and mixings in gauge models with spontaneous parity violation, Phys. Rev. D **23**, 165 (1981).
[6] M. Magg and C. Wetterich, Neutrino mass problem and gauge hierarchy, Phys. Lett. **94B**, 61 (1980).
[7] S. Weinberg, Baryon and Lepton Nonconserving Processes, Phys. Rev. Lett. **43**, 1566 (1979).
[8] E. Ma, Pathways to Naturally Small Neutrino Masses, Phys. Rev. Lett. **81**, 1171 (1998).
[9] K. Huitu, J. Maalampi, A. Pietila, and M. Raidal, Doubly charged Higgs at LHC, Nucl. Phys. **B487**, 27 (1997).
[10] J. F. Gunion, C. Loomis, and K. T. Pitts, Searching for doubly charged Higgs bosons at future colliders, eConf **C960625**, LTH096 (1996).
[11] S. Chakrabarti, D. Choudhury, R. M. Godbole, and B. Mukhopadhyaya, Observing doubly charged Higgs bosons in photon-photon collisions, Phys. Lett. B **434**, 347 (1998).
[12] M. Muhlleitner and M. Spira, A note on doubly charged Higgs pair production at hadron colliders, Phys. Rev. D **68**, 117701 (2003).
[13] A. G. Akeroyd and M. Aoki, Single and pair production of doubly charged Higgs bosons at hadron colliders, Phys. Rev. D **72**, 035011 (2005).
[14] T. Han, B. Mukhopadhyaya, Z. Si, and K. Wang, Pair production of doubly charged scalars: Neutrino mass

constraints and signals at the LHC, Phys. Rev. D **76**, 075013 (2007).
[15] J. Garayoa and T. Schwetz, Neutrino mass hierarchy and Majorana *CP* phases within the Higgs triplet model at the LHC, J. High Energy Phys. 03 (2008) 009.
[16] F. del Aguila and J. A. Aguilar-Saavedra, Distinguishing seesaw models at LHC with multi-lepton signals, Nucl. Phys. **B813**, 22 (2009).
[17] P. Fileviez Perez, T. Han, G.-y. Huang, T. Li, and K. Wang, Neutrino masses and the CERN LHC: Testing type II seesaw, Phys. Rev. D **78**, 015018 (2008).
[18] A. G. Akeroyd and C.-W. Chiang, Doubly charged Higgs bosons and three-lepton signatures in the Higgs Triplet Model, Phys. Rev. D **80**, 113010 (2009).
[19] A. G. Akeroyd, C.-W. Chiang, and N. Gaur, Leptonic signatures of doubly charged Higgs boson production at the LHC, J. High Energy Phys. 11 (2010) 005.
[20] A. Melfo, M. Nemevsek, F. Nesti, G. Senjanovic, and Y. Zhang, Type II seesaw at LHC: The roadmap, Phys. Rev. D **85**, 055018 (2012).
[21] M. Aoki, S. Kanemura, and K. Yagyu, Testing the Higgs triplet model with the mass difference at the LHC, Phys. Rev. D **85**, 055007 (2012).
[22] A. G. Akeroyd and H. Sugiyama, Production of doubly charged scalars from the decay of singly charged scalars in the Higgs Triplet Model, Phys. Rev. D **84**, 035010 (2011).
[23] C.-W. Chiang, T. Nomura, and K. Tsumura, Search for doubly charged Higgs bosons using the same-sign diboson mode at the LHC, Phys. Rev. D **85**, 095023 (2012).
[24] A. G. Akeroyd, S. Moretti, and H. Sugiyama, Five-lepton and six-lepton signatures from production of neutral triplet scalars in the Higgs Triplet Model, Phys. Rev. D **85**, 055026 (2012).
[25] E. J. Chun and P. Sharma, Same-sign tetra-leptons from type II seesaw, J. High Energy Phys. 08 (2012) 162.
[26] F. del Águila and M. Chala, LHC bounds on lepton number violation mediated by doubly and singly charged scalars, J. High Energy Phys. 03 (2014) 027.
[27] E. J. Chun and P. Sharma, Search for a doubly charged boson in four lepton final states in type II seesaw, Phys. Lett. B **728**, 256 (2014).
[28] S. Kanemura, K. Yagyu, and H. Yokoya, First constraint on the mass of doubly charged Higgs bosons in the same-sign diboson decay scenario at the LHC, Phys. Lett. B **726**, 316 (2013).
[29] S. Kanemura, M. Kikuchi, K. Yagyu, and H. Yokoya, Bounds on the mass of doubly charged Higgs bosons in the same-sign diboson decay scenario, Phys. Rev. D **90**, 115018 (2014).
[30] S. Kanemura, M. Kikuchi, H. Yokoya, and K. Yagyu, LHC Run-I constraint on the mass of doubly charged Higgs bosons in the same-sign diboson decay scenario, Prog. Theor. Exp. Phys. **2015**, 051B02 (2015).
[31] Z. Kang, J. Li, T. Li, Y. Liu, and G.-Z. Ning, Light doubly charged Higgs boson via the WW^* channel at LHC, Eur. Phys. J. C **75**, 574 (2015).
[32] Z.-L. Han, R. Ding, and Y. Liao, LHC phenomenology of type II seesaw: Nondegenerate case, Phys. Rev. D **91**, 093006 (2015).
[33] Z.-L. Han, R. Ding, and Y. Liao, LHC phenomenology of the type II seesaw mechanism: Observability of neutral scalars in the nondegenerate case, Phys. Rev. D **92**, 033014 (2015).
[34] M. Mitra, S. Niyogi, and M. Spannowsky, Type II seesaw model and multilepton signatures at hadron colliders, Phys. Rev. D **95**, 035042 (2017).
[35] D. K. Ghosh, N. Ghosh, I. Saha, and A. Shaw, Revisiting the high-scale validity of the type II seesaw model with novel LHC signature, Phys. Rev. D **97**, 115022 (2018).
[36] S. Antusch, O. Fischer, A. Hammad, and C. Scherb, Low scale type II seesaw: Present constraints and prospects for displaced vertex searches, J. High Energy Phys. 02 (2019) 157.
[37] P. S. Bhupal Dev and Y. Zhang, Displaced vertex signatures of doubly charged scalars in the type II seesaw and its left-right extensions, J. High Energy Phys. 10 (2018) 199.
[38] T. B. de Melo, F. S. Queiroz, and Y. Villamizar, Doubly charged scalar at the high-luminosity and high-energy LHC, Int. J. Mod. Phys. A **34**, 1950157 (2019).
[39] R. Primulando, J. Julio, and P. Uttayarat, Scalar phenomenology in type II seesaw model, J. High Energy Phys. 08 (2019) 024.
[40] E. J. Chun, S. Khan, S. Mandal, M. Mitra, and S. Shil, Same-sign tetralepton signature at the Large Hadron Collider and a future pp collider, Phys. Rev. D **101**, 075008 (2020).
[41] R. Padhan, D. Das, M. Mitra, and A. Kumar Nayak, Probing doubly and singly charged Higgs bosons at the pp collider HE-LHC, Phys. Rev. D **101**, 075050 (2020).
[42] S. Ashanujjaman and K. Ghosh, Revisiting type II seesaw: Present limits and future prospects at LHC, J. High Energy Phys. 03 (2022) 195.
[43] T. Nomura, H. Okada, and H. Yokoya, Discriminating leptonic Yukawa interactions with doubly charged scalar at the ILC, Nucl. Phys. **B929**, 193 (2018).
[44] S. Blunier, G. Cottin, M. A. Díaz, and B. Koch, Phenomenology of a Higgs triplet model at future e^+e^- colliders, Phys. Rev. D **95**, 075038 (2017).
[45] A. Crivellin, M. Ghezzi, L. Panizzi, G. M. Pruna, and A. Signer, Low- and high-energy phenomenology of a doubly charged scalar, Phys. Rev. D **99**, 035004 (2019).
[46] P. Agrawal, M. Mitra, S. Niyogi, S. Shil, and M. Spannowsky, Probing the type II seesaw mechanism through the production of Higgs bosons at a lepton collider, Phys. Rev. D **98**, 015024 (2018).
[47] L. Rahili, A. Arhrib, and R. Benbrik, Associated production of SM Higgs with a photon in type II seesaw models at the ILC, Eur. Phys. J. C **79**, 940 (2019).
[48] P. Bandyopadhyay, A. Karan, and C. Sen, Discerning signatures of seesaw models and complementarity of leptonic colliders, arXiv:2011.04191.
[49] P. S. B. Dev, S. Khan, M. Mitra, and S. K. Rai, Doubly charged Higgs boson at a future electron-proton collider, Phys. Rev. D **99**, 115015 (2019).
[50] X.-H. Yang and Z.-J. Yang, Doubly charged Higgs production at future ep colliders, Chin. Phys. C **46**, 063107 (2022).

[51] F. F. Deppisch, P. S. Bhupal Dev, and A. Pilaftsis, Neutrinos and collider physics, New J. Phys. **17**, 075019 (2015).
[52] Y. Cai, T. Han, T. Li, and R. Ruiz, Lepton number violation: Seesaw models and their collider tests, Front. Phys. **6**, 40 (2018).
[53] G. Aad *et al.* (ATLAS Collaboration), Search for doubly charged Higgs bosons in like-sign dilepton final states at $\sqrt{s} = 7$ TeV with the ATLAS detector, Eur. Phys. J. C **72**, 2244 (2012).
[54] S. Chatrchyan *et al.* (CMS Collaboration), A search for a doubly charged Higgs boson in pp collisions at $\sqrt{s} = 7$ TeV, Eur. Phys. J. C **72**, 2189 (2012).
[55] G. Aad *et al.* (ATLAS Collaboration), Search for anomalous production of prompt same-sign lepton pairs and pair-produced doubly charged Higgs bosons with $\sqrt{s} = 8$ TeV pp collisions using the ATLAS detector, J. High Energy Phys. 03 (2015) 041.
[56] V. Khachatryan *et al.* (CMS Collaboration), Study of Vector Boson Scattering and Search for New Physics in Events with Two Same-Sign Leptons and Two Jets, Phys. Rev. Lett. **114**, 051801 (2015).
[57] CMS Collaboration, Search for a doubly charged Higgs boson with $\sqrt{s} = 8$ TeV pp collisions at the CMS experiment, Report No. CMS-PAS-HIG-14-039 (2016), http://cds.cern.ch/record/2127498.
[58] CMS Collaboration, A search for doubly charged Higgs boson production in three and four lepton final states at $\sqrt{s} = 13$ TeV, Report No. CMS-PAS-HIG-16-036 (2017), https://cds.cern.ch/record/2242956.
[59] M. Aaboud *et al.* (ATLAS Collaboration), Search for doubly charged Higgs boson production in multi-lepton final states with the ATLAS detector using proton–proton collisions at $\sqrt{s} = 13$ TeV, Eur. Phys. J. C **78**, 199 (2018).
[60] A. M. Sirunyan *et al.* (CMS Collaboration), Observation of Electroweak Production of Same-Sign W Boson Pairs in the Two Jet and Two Same-Sign Lepton Final State in Proton-Proton Collisions at $\sqrt{s} = 13$ TeV, Phys. Rev. Lett. **120**, 081801 (2018).
[61] M. Aaboud *et al.* (ATLAS Collaboration), Search for doubly charged scalar bosons decaying into same-sign W boson pairs with the ATLAS detector, Eur. Phys. J. C **79**, 58 (2019).
[62] G. Aad *et al.* (ATLAS Collaboration), Search for doubly and singly charged Higgs bosons decaying into vector bosons in multi-lepton final states with the ATLAS detector using proton-proton collisions at $\sqrt{s} = 13$ TeV, J. High Energy Phys. 06 (2021) 146.
[63] G. Aad *et al.* (ATLAS Collaboration), Combination of searches for Higgs boson pairs in pp collisions at $\sqrt{s} =$ 13 TeV with the ATLAS detector, Phys. Lett. B **800**, 135103 (2020).
[64] G. Aad *et al.* (ATLAS Collaboration), Search for high-mass dilepton resonances using 139 fb^{-1} of pp collision data collected at $\sqrt{s} = 13$ TeV with the ATLAS detector, Phys. Lett. B **796**, 68 (2019).
[65] G. Aad *et al.* (ATLAS Collaboration), Search for diboson resonances in hadronic final states in 139 fb^{-1} of pp collisions at $\sqrt{s} = 13$ TeV with the ATLAS detector, J. High Energy Phys. 09 (2019) 091; J. High Energy Phys. 06 (2020) 042(E).
[66] G. Aad *et al.* (ATLAS Collaboration), Search for a heavy charged boson in events with a charged lepton and missing transverse momentum from pp collisions at $\sqrt{s} = 13$ TeV with the ATLAS detector, Phys. Rev. D **100**, 052013 (2019).
[67] G. Aad *et al.* (ATLAS Collaboration), Search for heavy resonances decaying into a pair of Z bosons in the $\ell^+\ell^-\ell'^+\ell'^-$ and $\ell^+\ell^-\nu\bar{\nu}$ final states using 139 fb^{-1} of proton–proton collisions at $\sqrt{s} = 13$ TeV with the ATLAS detector, Eur. Phys. J. C **81**, 332 (2021).
[68] G. Aad *et al.* (ATLAS Collaboration), Search for heavy diboson resonances in semileptonic final states in pp collisions at $\sqrt{s} = 13$ TeV with the ATLAS detector, Eur. Phys. J. C **80**, 1165 (2020).
[69] G. Aad *et al.* (ATLAS Collaboration), Search for a heavy Higgs boson decaying into a Z boson and another heavy Higgs boson in the $\ell\ell bb$ and $\ell\ell WW$ final states in pp collisions at $\sqrt{s} = 13$ TeV with the ATLAS detector, Eur. Phys. J. C **81**, 396 (2021).
[70] ATLAS Collaboration, Search for heavy resonances decaying into a Z boson and a Higgs boson in final states with leptons and b-jets in 139 fb^{-1} of pp collisions at $\sqrt{s} = 13$ TeV with the ATLAS detector, Report No. ATLAS-CONF-2020-043 (2020), https://cds.cern.ch/record/2728053.
[71] G. Aad *et al.* (ATLAS Collaboration), Search for resonances decaying into a weak vector boson and a Higgs boson in the fully hadronic final state produced in proton-proton collisions at $\sqrt{s} = 13$ TeV with the ATLAS detector, Phys. Rev. D **102**, 112008 (2020).
[72] ATLAS Collaboration, Search for heavy resonances decaying into a W boson and a Higgs boson in final states with leptons and b-jets in 139 fb^{-1} of pp collisions at $\sqrt{s} = 13$ TeV with the ATLAS detector, Report No. ATLAS-CONF-2021-026 (2021), http://cds.cern.ch/record/2773302.
[73] G. Aad *et al.* (ATLAS Collaboration), Search for resonances decaying into photon pairs in 139 fb^{-1} of pp collisions at $\sqrt{s} = 13$ TeV with the ATLAS detector, Phys. Lett. B **822**, 136651 (2021).
[74] ATLAS Collaboration, Search for high-mass resonances in final states with a tau lepton and missing transverse momentum with the ATLAS detector, Report No. ATLAS-CONF-2021-025 (2021), http://cds.cern.ch/record/2773301.
[75] A. Tumasyan *et al.* (CMS Collaboration), Search for heavy resonances decaying to WW, WZ, or WH boson pairs in the lepton plus merged jet final state in proton-proton collisions at $\sqrt{s} = 13$ TeV, Phys. Rev. D **105**, 032008 (2022).
[76] A. Tumasyan *et al.* (CMS Collaboration), Search for heavy resonances decaying to a pair of Lorentz-boosted Higgs bosons in final states with leptons and a bottom quark pair at $\sqrt{s} = 13$ TeV, J. High Energy Phys. 05 (2022) 005.
[77] A. Tumasyan *et al.* (CMS Collaboration), Search for heavy resonances decaying to ZZ or ZW and axion-like particles

mediating nonresonant ZZ or ZH production at $\sqrt{s} =$ 13 TeV, J. High Energy Phys. 04 (2022) 087.
[78] ATLAS Collaboration, Combination of searches for heavy resonances using 139 fb^{-1} of proton–proton collision data at $\sqrt{s} = 13$ TeV with the ATLAS detector, Report No. ATLAS-CONF-2022-028 (2022), http://cds.cern.ch/record/2809967.
[79] G. Aad *et al.* (ATLAS Collaboration), Search for resonant pair production of Higgs bosons in the $b\bar{b}b\bar{b}$ final state using pp collisions at $\sqrt{s} = 13$ TeV with the ATLAS detector, Phys. Rev. D **105**, 092002 (2022).
[80] ATLAS Collaboration, Search for heavy resonances decaying into a Z or W boson and a Higgs boson in final states with leptons and b-jets in 139 fb^{-1} of pp collisions at $\sqrt{s} = 13$ TeV with the ATLAS detector, arXiv:2207.00230.
[81] P. Fileviez Perez, T. Han, G.-y. Huang, T. Li, and K. Wang, Neutrino masses and the CERN LHC: Testing type II seesaw, Phys. Rev. D **78**, 015018 (2008).
[82] A. Arhrib, R. Benbrik, M. Chabab, G. Moultaka, M. C. Peyranere, L. Rahili, and J. Ramadan, The Higgs potential in the type II seesaw model, Phys. Rev. D **84**, 095005 (2011).
[83] E. Accomando *et al.* (CLIC Physics Working Group), Physics at the CLIC multi-TeV linear collider, in *Proceedings of the 11th International Conference on Hadron Spectroscopy*, CERN Yellow Reports: Monographs (CERN, Geneva, 2004), p. 226, arXiv:hep-ph/0412251, http://cds.cern.ch/record/749219.
[84] The international linear collider technical design report—volume 2: Physics, arXiv:1306.6352.
[85] A. Abada *et al.* (FCC Collaboration), FCC-ee: The lepton collider: Future circular collider conceptual design report volume 2, Eur. Phys. J. Special Topics **228**, 261 (2019).
[86] M. Dong *et al.* (CEPC Study Group), CEPC conceptual design report: Volume 2—physics & detector, arXiv:1811.10545.
[87] I. Esteban, M. C. Gonzalez-Garcia, M. Maltoni, T. Schwetz, and A. Zhou, The fate of hints: Updated global analysis of three-flavor neutrino oscillations, J. High Energy Phys. 09 (2020) 178.
[88] P. A. Zyla *et al.* (Particle Data Group), Review of particle physics, Prog. Theor. Exp. Phys. **2020**, 083C01 (2020).
[89] M. Aoki, S. Kanemura, M. Kikuchi, and K. Yagyu, Radiative corrections to the Higgs boson couplings in the triplet model, Phys. Rev. D **87**, 015012 (2013).
[90] E. J. Chun, H. M. Lee, and P. Sharma, Vacuum Stability, Perturbativity, EWPD and Higgs-to-diphoton rate in type II seesaw models, J. High Energy Phys. 11 (2012) 106.
[91] D. Das and A. Santamaria, Updated scalar sector constraints in the Higgs triplet model, Phys. Rev. D **94**, 015015 (2016).
[92] A. M. Baldini *et al.* (MEG Collaboration), Search for the lepton flavour violating decay $\mu^+ \to \text{e}^+\gamma$ with the full dataset of the MEG experiment, Eur. Phys. J. C **76**, 434 (2016).
[93] U. Bellgardt *et al.* (SINDRUM Collaboration), Search for the decay $\mu^+ \text{—>} e^+ e^+ e^-$, Nucl. Phys. **B299**, 1 (1988).
[94] M. Kakizaki, Y. Ogura, and F. Shima, Lepton flavor violation in the triplet Higgs model, Phys. Lett. B **566**, 210 (2003).
[95] A. G. Akeroyd, M. Aoki, and H. Sugiyama, Lepton flavor violating decays τ—> anti-l ll and μ—> e gamma in the Higgs triplet model, Phys. Rev. D **79**, 113010 (2009).
[96] D. N. Dinh, A. Ibarra, E. Molinaro, and S. T. Petcov, The $\mu - e$ conversion in nuclei, $\mu \to e\gamma$, $\mu \to 3e$ decays and TeV scale seesaw scenarios of neutrino mass generation, J. High Energy Phys. 08 (2012) 125; J. High Energy Phys. 09 (2013) 023(E).
[97] F. Staub, SARAH 4: A tool for (not only SUSY) model builders, Comput. Phys. Commun. **185**, 1773 (2014).
[98] F. Staub, Exploring new models in all detail with SARAH, Adv. High Energy Phys. **2015**, 840780 (2015).
[99] C. Degrande, C. Duhr, B. Fuks, D. Grellscheid, O. Mattelaer, and T. Reiter, UFO—The Universal FeynRules Output, Comput. Phys. Commun. **183**, 1201 (2012).
[100] J. Alwall, M. Herquet, F. Maltoni, O. Mattelaer, and T. Stelzer, MadGraph 5: Going beyond, J. High Energy Phys. 06 (2011) 128.
[101] J. Alwall, R. Frederix, S. Frixione, V. Hirschi, F. Maltoni, O. Mattelaer, H. S. Shao, T. Stelzer, P. Torrielli, and M. Zaro, The automated computation of tree-level and next-to-leading order differential cross sections, and their matching to parton shower simulations, J. High Energy Phys. 07 (2014) 079.
[102] T. Sjöstrand, S. Ask, J. R. Christiansen, R. Corke, N. Desai, P. Ilten, S. Mrenna, S. Prestel, C. O. Rasmussen, and P. Z. Skands, An introduction to PYTHIA 8.2, Comput. Phys. Commun. **191**, 159 (2015).
[103] J. de Favereau, C. Delaere, P. Demin, A. Giammanco, V. Lemaître, A. Mertens, and M. Selvaggi (DELPHES 3 Collaboration), DELPHES 3, A modular framework for fast simulation of a generic collider experiment, J. High Energy Phys. 02 (2014) 057.
[104] M. Cacciari, G. P. Salam, and G. Soyez, The anti-k_t jet clustering algorithm, J. High Energy Phys. 04 (2008) 063.
[105] M. Cacciari, G. P. Salam, and G. Soyez, FastJet user manual, Eur. Phys. J. C **72**, 1896 (2012).
[106] M. Aaboud *et al.* (ATLAS Collaboration), Top-quark mass measurement in the all-hadronic $t\bar{t}$ decay channel at $\sqrt{s} =$ 8 TeV with the ATLAS detector, J. High Energy Phys. 09 (2017) 118.
[107] A. M. Sirunyan *et al.* (CMS Collaboration), Measurement of the top quark mass in the all-jets final state at $\sqrt{s} =$ 13 TeV and combination with the lepton + jets channel, Eur. Phys. J. C **79**, 313 (2019).
[108] G. Aad *et al.* (ATLAS Collaboration), Measurements of top-quark pair single- and double-differential cross sections in the all-hadronic channel in pp collisions at $\sqrt{s} =$ 13 TeV using the ATLAS detector, J. High Energy Phys. 01 (2021) 033.
[109] K. Cranmer, Profile likelihood number counting combination (2007), http://physstat.org/physstat/packages/0803001.1.html.
[110] W. Verkerke and D. P. Kirkby, The RooFit toolkit for data modeling, eConf **C0303241**, MOLT007 (2003).

[111] R. Brun and F. Rademakers, ROOT: An object oriented data analysis framework, Nucl. Instrum. Methods Phys. Res., Sect. A **389**, 81 (1997).
[112] I. Smiljanic, I. B. Jelisavcic, G. Kacarevic, N. Vukasinovic, I. Vidakovic, and V. Rekovic, Systematic uncertainties in integrated luminosity measurement at CEPC, J. Instrum. **17**, P09014 (2022).
[113] I. Bozovic-Jelisavcic, H. Abramowicz, P. Bambade, T. Jovin, M. Pandurovic, B. Pawlik, C. Rimbault, I. Sadeh, and I. Smiljanic, Luminosity measurement at ILC, arXiv: 1006.2539.
[114] G. Tang *et al.*, The circular electron–positron collider beam energy measurement with Compton scattering and beam tracking method, Rev. Sci. Instrum. **91**, 033109 (2020).
[115] M. Si *et al.*, High energy beam energy measurement with microwave–electron Compton backscattering, Nucl. Instrum. Methods Phys. Res., Sect. A **1026**, 166216 (2022).
[116] D. Xu, Y.-S. Huang, G.-Y. Tang, S.-H. Chen, M.-Y. Si, and J.-Y. Zhang, Circular electron-positron collider beam energy measurement scheme based on microwave-electronic Compton backscattering, Acta Phys. Sin. **70**, 131301 (2021).
[117] A. Heister *et al.* (ALEPH Collaboration), Search for scalar leptons in $e^+ e^-$ collisions at center-of-mass energies up to 209-GeV, Phys. Lett. B **526**, 206 (2002).
[118] J. Abdallah *et al.* (DELPHI Collaboration), Searches for supersymmetric particles in $e^+ e^-$ collisions up to 208-GeV and interpretation of the results within the MSSM, Eur. Phys. J. C **31**, 421 (2003).
[119] G. Abbiendi *et al.* (OPAL Collaboration), Search for anomalous production of dilepton events with missing transverse momentum in $e^+ e^-$ collisions at $\sqrt{s} =$ 183-Gev to 209-GeV, Eur. Phys. J. C **32**, 453 (2004).
[120] J. Yuan, H. Cheng, and X. Zhuang, Prospects for slepton pair production in the future $e^- e^+$ Higgs factories, arXiv: 2203.10580.
[121] J.-R. Yuan, H.-J. Cheng, and X.-A. Zhuang, Prospects for chargino pair production at the CEPC *, Chin. Phys. C **46**, 013104 (2022).